npj | Clean Water

www.nature.com/npjcleanwater

ARTICLE OPEN

Effect of pre-coagulation using different aluminium species on crystallization of cake layer and membrane fouling

Wenzheng Yu[1,2], Mengjie Liu[1], Xuejia Zhang[1], Nigel Graham[2] and Jiuhui Qu[1]

Pre-coagulation could mitigate the membrane fouling, and thus we used different Al coagulants as a pre-treatment for ultrafiltration to explore their effects on the morphology of the membrane cake layer and fouling. Parallel bench-scale tests, using three different species of Al ($AlCl_3$, $PACl_{15}$, and $PACl_{25}$), with and without humic acid, were operated continuously for a long period to investigate the effects of floc aging (~13 days). Specifically, the presence of humic acid affects the cake layer by influencing the rate and extent of floc crystallization, as greater crystallization leads to greater fouling (bio-fouling was excluded in this study). The fouling rate (indicated by the trans-membrane pressure at constant flux) varied with Al species and was found to increase as follows: $PACl_{15}$ < $PACl_{25}$ < $AlCl_3$. The presence of humic acid also intensify membrane flouling. The results showed that three species of Al induced different sizes of primary nanoparticles and fractal dimensions of flocs, and therefore produced cake layers with different thickness/structure. Analysis of flocs with different ages indicated a crystallization process in the cake layer. Crystallization exacerbate membrane fouling by decreasing the porosity of the cake layer, and the situation became severe in the presence of humic acid.

npj Clean Water (2019)2:17 ; https://doi.org/10.1038/s41545-019-0040-3

INTRODUCTION

Different types of pre-treatment before membrane filtration have been explored for many years, such as adsorption, coagulation, and oxidation.[1–4] Some materials, such as powdered activated carbon (PAC),[5] heated aluminum oxide particles (HAOPs),[6,7] magnetic ion exchange (MIEX)[8] and synthesized zeolite,[9] have been studied as pre-adsorption materials to mitigate membrane fouling. An anion exchange resin before ultrafiltration can also significantly mitigate irreversible fouling and reduce the dissolved organic carbon (DOC) content of clarified water.[10] The principal purpose of these alternative adsorption methods is to remove problematic contaminants before they reach the membrane surface, and cause significant fouling effects.

In addition to adsorption, chemical coagulation as a pre-treatment for membrane filtration can mitigate microfiltration (MF) or ultrafiltration (UF) membrane fouling for drinking water treatment, removing most of the turbidity, microorganisms, biopolymers and 30–40% of dissolved organic matter.[11–15] Pre-coagulation by alum, ferric salts and other developed coagulants can extenuate irreversible membrane fouling in the treatment of wastewater[16–18] and wastewater effluent.[19,20] Lahoussine-Turcaud et al.[21] found that polyaluminium chloride could reduce the fouling rate polysulfone UF membrane for river water treatment, but co-addition of organic polymers and polyferric chloride may cause greater membrane fouling.[22]

Therefore, the permeate flux of a membrane is influenced by the kind of coagulant(s) used in the pre-treatment.[23] In addition, a previous study demonstrated that the treatment performance decreased with the type of coagulant in the following order: $Al_2(SO_4)_3$ > $Fe_2(SO_4)_3$ > $FeCl_3$.[24] Citulski et al.[25] found that alum caused negligible irreversible fouling and stabilized the reversible fouling rate, while ferric chloride caused rapid and irreversible fouling. A comparison among $Al_2(SO_4)_3$, $NaAlO_2$, and polyaluminum chloride (PACl) suggested that using sodium aluminate as coagulant resulted in less organic matter removal and a considerable residual aluminum concentration after the coagulation process, as well as with coagulation combined with an ultrafiltration process.[26]

When using aluminum-based coagulants, the structure of the flocs is determined by the species of Al, which influences the properties of the cake layer, and thus the behavior of the membrane filter.[27] Precipitates formed from polyaluminum chloride (PACl) were reported to cause more irreversible fouling than those formed from the monomeric aluminum coagulants,[28] and it was found that PACl–Al_b (medium polynuclear Al species) caused the greatest flux decline.[29,30] However, it is noted that these experiments relating to drinking water treatment were carried out with flat membranes, which may necessarily accurately predict the behavior of hollow fiber membrane applications.

Generally, pore blocking, adsorption, and cake formation are three kinds of mechanisms that caused membrane fouling, as well as flux decline.[31] While considerable research has been conducted on the pre-coagulation performance with different coagulants, as indicated above, the mechanisms of membrane fouling have not been fully established. Some previous studies by others[32] and in our research[33] have suggested that cake formation was the predominant mechanism of membrane fouling, as well as the presence of biopolymers. Other studies have indicated that the physico-chemistry and structure of the coagulated flocs, and thus the porosity of cake layer, were an important influence on filtration efficiency.[34–37]

Precipitated amorphous metal hydroxide slowly transforms into a crystalline form as it ages.[38] During this process, large amounts of water in the freshly precipitated hydroxide are released, which

[1]Key Laboratory of Drinking Water Science and Technology, Research Center for Eco-Environmental Sciences, Chinese Academy of Sciences, Beijing 100085, China and [2]Department of Civil and Environmental Engineering, Imperial College London, South Kensington Campus, London SW7 2AZ, UK
Correspondence: Wenzheng Yu (wzyu@rcees.ac.cn) or Nigel Graham (n.graham@imperial.ac.uk)

Received: 28 February 2019 Accepted: 23 July 2019
Published online: 14 August 2019

induces lattice re-organization and the formation of micro-crystals.[39,40] As shown by de Vicente et al.,[41] $Al(OH)_3$ precipitate lost 75% of its adsorption capacity for PO_4^{3-} after aging, and the reactivity of aluminum in the precipitate was found to steadily decrease.[42]

The aging environment strongly influences the process of crystallization, such as the transformation of amorphous alumina gels into pseudo-boehmite.[43] Particular components in solution impede/inhibit the crystallization of aluminum hydroxide,[42] such as carbonate, nitrate, chloride, and sulfate.[43,44] For ferrihydrite precipitate, the process of crystallization was found to be inhibited by Si.[45] Lin et al.[46] confirmed that the crystalline structure of the Al_{13} aggregates differed from that of $Al(OH)_3$ and that the Al_{13} aggregates did not have a well-defined crystalline structure.

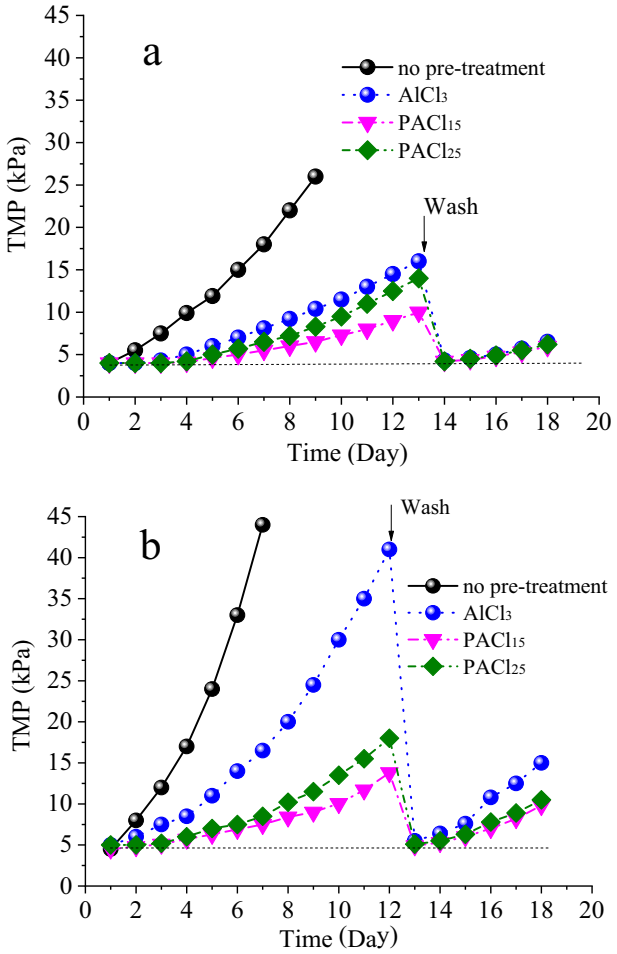

Fig. 1 Variation of TMP during the operation of the four pre-coagulation systems: **a** without HA, **b** with HA (the flux of the UF systems was maintained at 20 $Lm^{-2}h^{-1}$)

Therefore, the presence of background contaminants, such as organic matter, anions, etc., can influence the properties of coagulant precipitates or flocs, and thus alter the structure of the cake layer (formed by flocs) on membrane surfaces after long operation times (facilitating the crystallization process), and thereby induce different membrane fouling effects. Currently, there is a scarcity of information concerning the impact of floc crystallization on membrane fouling, and particularly the aging of hydroxide precipitate in the cake layer. In this paper, we have investigated the nature of the cake layers formed by different Al species, and the effect of humic acid (HA) on the process of crystallization in these layers, and the membrane fouling.

RESULTS AND DISCUSSION

TMP development in different systems

The variation of trans-membrane pressure (TMP) during the operation of ultrafiltration using $AlCl_3$, $PACl_{15}$, and $PACl_{25}$ as pre-coagulants is shown in Fig. 1, together with UF without pre-coagulant for comparison. The membrane system was operated for 13 days in the first phase, followed by a washing event to remove the cake layer from the membrane surface, and then the system was operated again for a further 5 days as a second phase (Fig. 1). The results show clearly that pre-coagulation mitigated the membrane fouling. While the development of TMP was significantly different in the four systems, from an initial value of ~5 kPa, the extent of fouling decreased in the order: no pre-treatmentå $AlCl_3$å $PACl_{25}$å $PACl_{15}$.

When HA was absent in the tap water (Fig. 1a), the TMP of the system without pre-coagulation started to increase immediately, while the TMP in other systems didn't start to increase until day 4. The values of TMP at the end of the first stage were 16kPa, 10kPa, and 14kPa for $AlCl_3$, $PACl_{15}$, and $PACl_{25}$ respectively. It can be seen that the TMP reduced to its initial value after washing at day 13 as the cake layers were removed in the three systems. For the tests with HA in the feed water, the TMP increased dramatically and the systems with pre-coagulation started to foul from the second day of operation. The values of TMP at day 13 were 42kPa, 14kPa, and 23 kPa for $AlCl_3$, $PACl_{15}$, and $PACl_{25}$ respectively, indicating that the presence of HA caused greater fouling. Since the TMP of the $AlCl_3$ coagulation-UF system increased rapidly in the presence of HA, it was evident that the addition of $AlCl_3$ was not an effective pre-treatment to alleviate the membrane fouling.

At the end of the first phase, the cake layer was cleaned by sponge washing for all four systems, and then the membrane systems were re-started. It was found that the TMP of all three membrane systems with pre-coagulation was again reduced to its initial value, indicating that the cleaning was effective with or without the presence of HA (Fig. 1). Therefore, the results showed that the cake layer dominated the membrane fouling in all systems, and the rapid growth of TMP in the HA-tap water tests suggested that the presence of HA affected the nature of the cake layer, causing a greater increase of membrane fouling. The results for TOC and UV_{254} (Tables 1 and 2) showed that the removal

Table 1. Water quality of influent and membrane filtrates for the coagulation-UF systems with tap water

Parameter	Raw water	$AlCl_3$-CUF filtrate	$PACl_{15}$-CUF filtrate	$PACl_{25}$-CUF filtrate
UV_{254} (cm^{-1})	0.330 ± 0.006	0.020 ± 0.003	0.019 ± 0.003	0.020 ± 0.003
TOC (mg/L)	2.29 ± 0.28	1.60 ± 0.11	1.56 ± 0.22	1.55 ± 0.22
Turbidity (NTU)	0.30 ± 0.16	0.08 ± 0.02	0.07 ± 0.02	0.06 ± 0.03
Residual Al (mg/L)	0.070 ± 0.002	0.095 ± 0.004	0.089 ± 0.003	0.093 ± 0.003
pH	7.86 ± 0.04	7.51 ± 0.02	7.80 ± 0.02	7.82 ± 0.01

For turbidity, UV_{254}, and TOC, the number of measurements $n = 7$; for residual Al, $n = 5$

Table 2. Water quality of influent and filtrates for the coagulation-UF systems with HA-tap water

Parameter	Raw water	$AlCl_3$-CUF filtrate	$PACl_{15}$-CUF filtrate	$PACl_{25}$-CUF filtrate
UV_{254} (cm^{-1})	0.124 ± 0.006	0.035 ± 0.003	0.029 ± 0.003	0.028 ± 0.003
TOC (mg/L)	4.182 ± 0.415	2.142 ± 0.234	2.268 ± 0.234	2.291 ± 0.287
Turbidity (NTU)	3.40 ± 0.16	0.06 ± 0.02	0.06 ± 0.03	0.07 ± 0.02
Al (mg/L)	0.070 ± 0.002	0.091 ± 0.002	0.084 ± 0.003	0.073 ± 0.003
pH	7.85 ± 0.06	7.51 ± 0.05	7.78 ± 0.05	7.83 ± 0.03

For turbidity, UV_{254}, and TOC, the number of measurements $n = 7$; for residual Al, $n = 5$

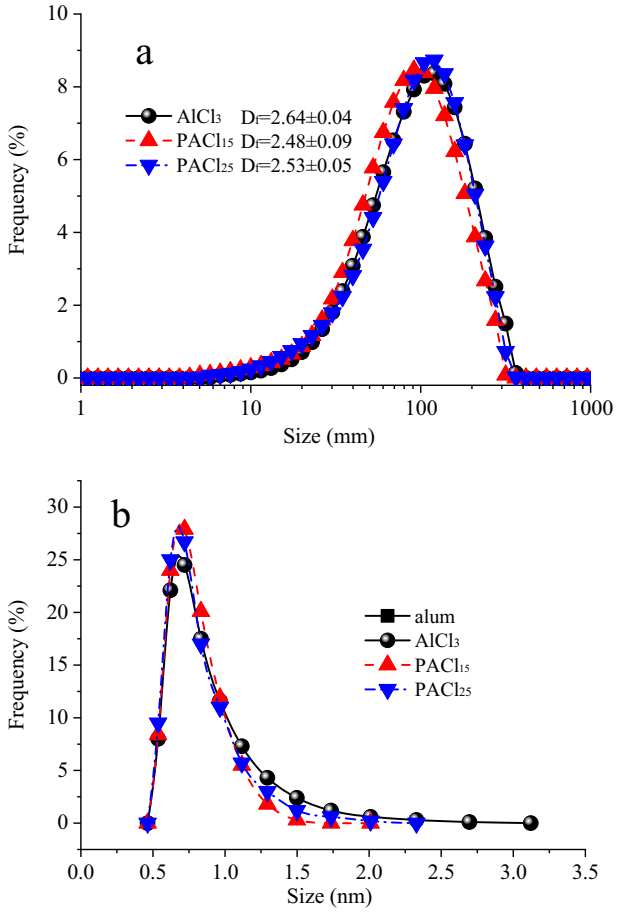

Fig. 2 Characteristics of Al-HA flocs in UF membrane tanks: **a** size distribution and fractal dimension of flocs (measured by Mastersizer 2000); **b** size distribution of particles after UF membrane filtration (measured by DLS)

efficiencies of organic matter in the three coagulation-UF systems were very similar. Therefore, it was concluded that the properties of the flocs forming the cake layer, were the main factor that influenced membrane fouling; this was investigated subsequently by reference to the size distribution and fractal dimension of flocs.

Structure of flocs and nano-scale primary particles

The particle (floc) size distribution (PSD) in the three membrane tanks, with different species of Al coagulants as pre-treatments, was measured by Mastersizer 2000 (Fig. 2). It can be seen that the PSD of flocs in all membrane tanks (Fig. 2a) was mainly between 5 and 300 μm, and there was little difference between them, although the PSD of the $PACl_{15}$ appeared to be slightly smaller than the $AlCl_3$ and $PACl_{25}$. The corresponding fractal dimension, D_f, of the $PACl_{15}$ was also the smallest of the three coagulant flocs, and the D_f values decreased in the order: $AlCl_3 > PACl_{25} > PACl_{15}$. From previous studies (e.g.[47]) it has been shown that, in general terms, the greater the fractal dimension, the more compact is the floc shape. Thus, the morphology of the cake layers in the three membrane systems are different as a consequence of the different floc sizes and shape/structure (fractal dimension). The results appear to indicate that the lowest rate of membrane fouling, with the $PACl_{15}$ coagulant, corresponded to a cake layer formed by flocs of a lower size and fractal dimension. The morphology of the cake layers will be discussed further with additional information provided by SEM images.

The possible involvement of nanoparticles (particles < 0.45 μm) in the membrane fouling process was investigated by determining the particle size distribution of solutions in the nano-scale range by DLS (Fig. 2b). It has been found by previous researchers that organic matter smaller than ~3 nm caused very little fouling.[48] Since the size distribution of the nanoparticles after 0.45 μm membrane was minor (<3 nm, Fig. 2b), it is probably that these smaller nanoparticles played little influence on the membrane fouling.

SEM image

SEM images of the cake layer for the three different membrane systems were compared (Figs. 3 and 4), and it was found that a thick cake layer formed on the membrane surface in all cases. However, the properties of the cake layers appeared to have significant differences between the three Al coagulants. For tap water in the absence of HA, all of the cake layers were found to consist of thousands of primary nanoparticles, and their average size varied between 20 and 30 nm (determined by Smileview software), which seemed to be determined by the Al species (B (OH/Al) value), as the size decreased as B value. The cake layer formed with $PACl_{15}$ precipitate had the highest porosity than the other two systems (determined by Smileview software), which confirmed with the result of Fig. 3.

In comparison to the tap water without HA, the properties of Al-HA cake layers on the fouled membrane (tap water with HA) seemed markedly different. While thick deposit layers were also formed on the surface of the fouled membranes, comprising colloidal material, the cake layers appeared more porous and the size of primary particles was larger compared to the tap water without HA. The images indicated the accumulation of flocs with primary nanoparticles of around 40, 40, and 30 nm for the $AlCl_3$, $PACl_{15}$, $PACl_{25}$ pre-coagulants (statistical results by software image J), respectively (Fig. 4a–c). According to filtration theory, the cake permeability should be greater where the constituent particles are larger. For the high increase of TMP by $AlCl_3$, it was probably related to the greater improvement of the crystalline of hydroxide flocs compared to the pre-formed Al coagulants ($PACl_{15}$ and $PACl_{25}$).

Apart from the size of the nanoparticles and the porosity of the cake layer, the thickness of cake layer also affected the external membrane fouling. Comparison of the thickness of the cake layer

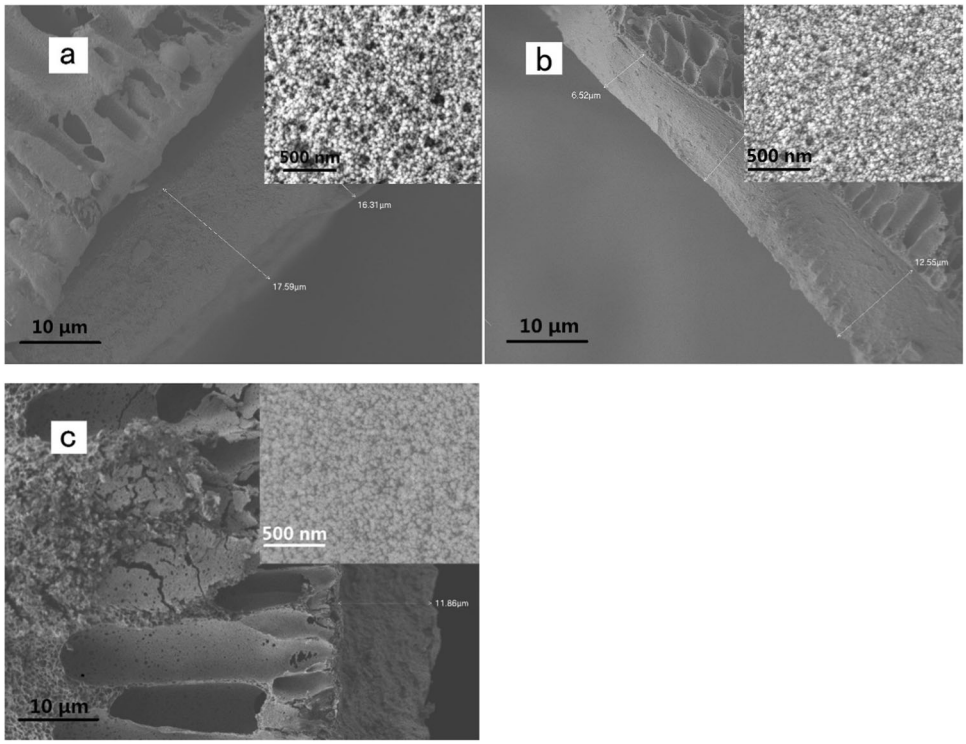

Fig. 3 SEM cross-section images of cake layer on the surface of membrane for different Al pre-coagulants *without* humic acid: **a** $AlCl_3$, **b** $PACl_{15}$, **c** $PACl_{25}$ (Insert images are the cake layer seen from the top)

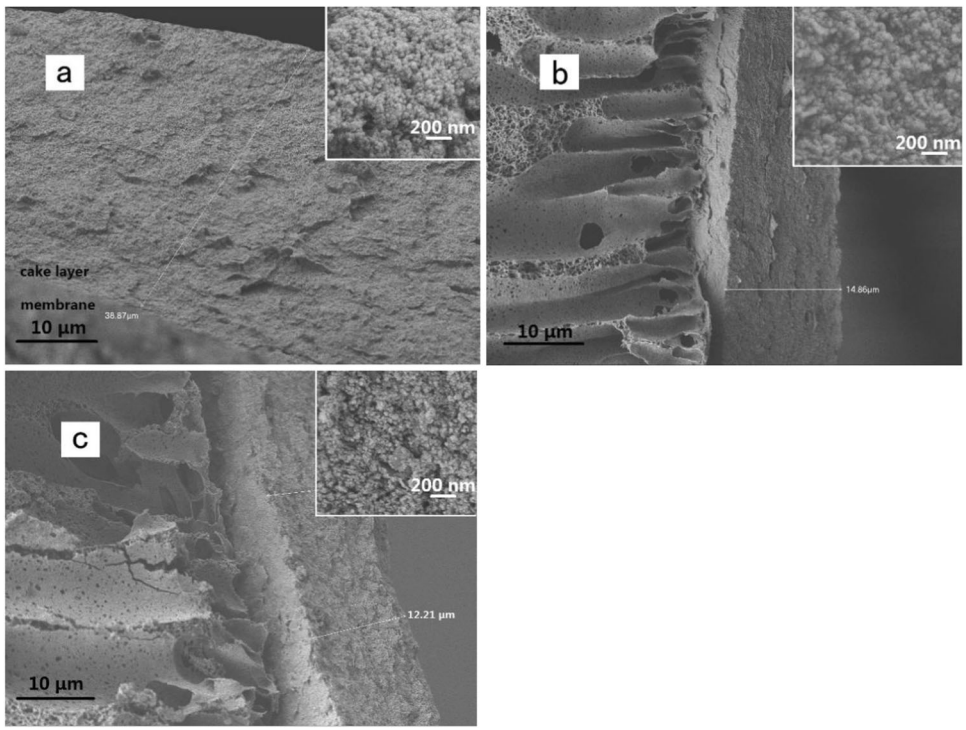

Fig. 4 SEM cross-section images of cake layer on the surface of membrane for different Al pre-coagulants *with* humic acid: **a** $AlCl_3$-humic; **b** $PACl_{15}$-humic; **c** $PACl_{25}$-humic (Insert images are the cake layer seen from the top)

for the different systems showed that the thickness decreased in the order: $AlCl_3 > PACl_{15} > PACl_{25}$. The cake layer with $PACl_{15}$ or $PACl_{25}$ flocs was arguably weaker due to charge neutralization, as $AlCl_3$ is more likely to form flocs as amorphous precipitates in sweep flocculation. Thus, the $PACl_{15}$ and $PACl_{25}$ cake layer may be easier to remove during the 1 min no suction between each 30 min filtration cycle. According to the results concerning the thickness and structure of cake layer, $PACl_{15}$ has the highest

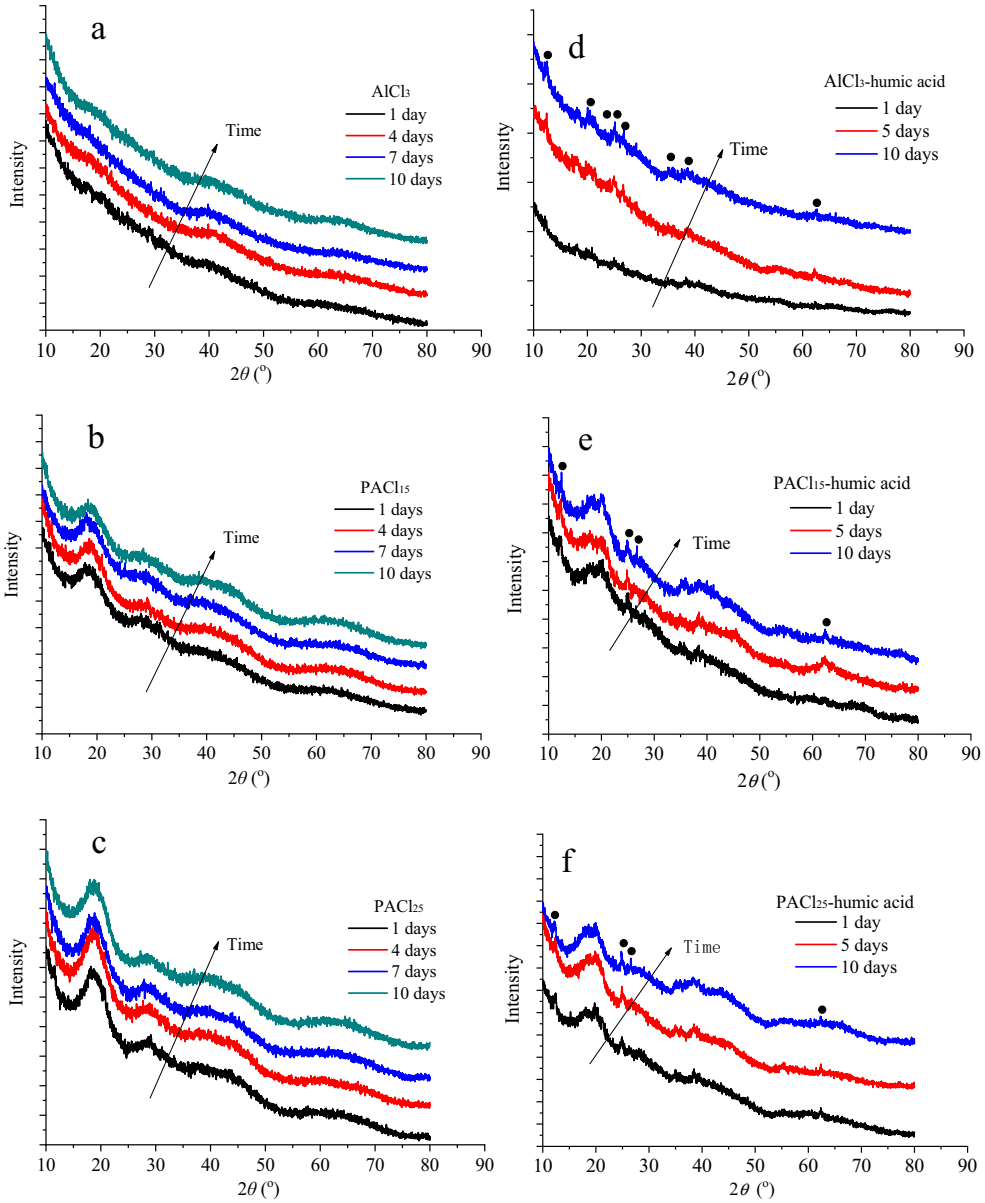

Fig. 5 Variation of XRD spectra of sludge (flocs) without/with HA for different ages: **a** $AlCl_3$ sludge, **b** $PACl_{15}$ sludge, **c** $PACl_{25}$ sludge, **d** $AlCl_3$-humic sludge, **e** $PACl_{15}$-humic sludge, **f** $PACl_{25}$-humic sludge

porosity and lowest thickness, which corresponded to the lowest degree of membrane fouling.

The flocs is of micron size, comprising nanoparticles whose size is larger than 20 nm. Therefore, it wouldn't induce complete pore blocking and further cause membrane fouling. It is suggested that cake formation is the dominating reason for membrane fouling here, as most of fouling could be removed by physical cleaning. However, the irreversible membrane fouling increased continuously, which might be attributed to the adsorption of organic matters escaped from the cake layer after crystallization or the ones from original water. Therefore, the influence of floc (cake layer) age was investigated, and specifically the process of crystallization of the flocs within the cake layer.

Crystallization of different aged flocs

The properties of flocs/cake layers with/without HA vary with time through the process of floc crystallization, which may cause greater membrane fouling. To consider this phenomenon, the crystallization of differently aged Al precipitates and Al-HA flocs (sludge) was examined by XRD (Fig. 5). As it was difficult to separate differently aged cake layers on the surface of the membrane, different depths (with different age) of the sludge in the UF tanks were used to instead to represent the differently aged cake layers, to investigate the extent of the crystallization.

XRD analysis of the sludges without HA, collected with different ages, showed a broad range of peaks and confirmed the presence of amorphous $Al(OH)_3$ with poorly ordered structure, especially for the polymeric Al (Fig. 5). Also, the XRD results for the Al precipitate sludges (without HA) showed that there were some differences between the three Al-coagulants. There was no broad peak for $AlCl_3$ sludge (monomer Al), while for the polymeric Al the intensity of the broad peaks increased as the B (OH/Al) value increased, which may be related to the existence of Al_{13}. It was evident that

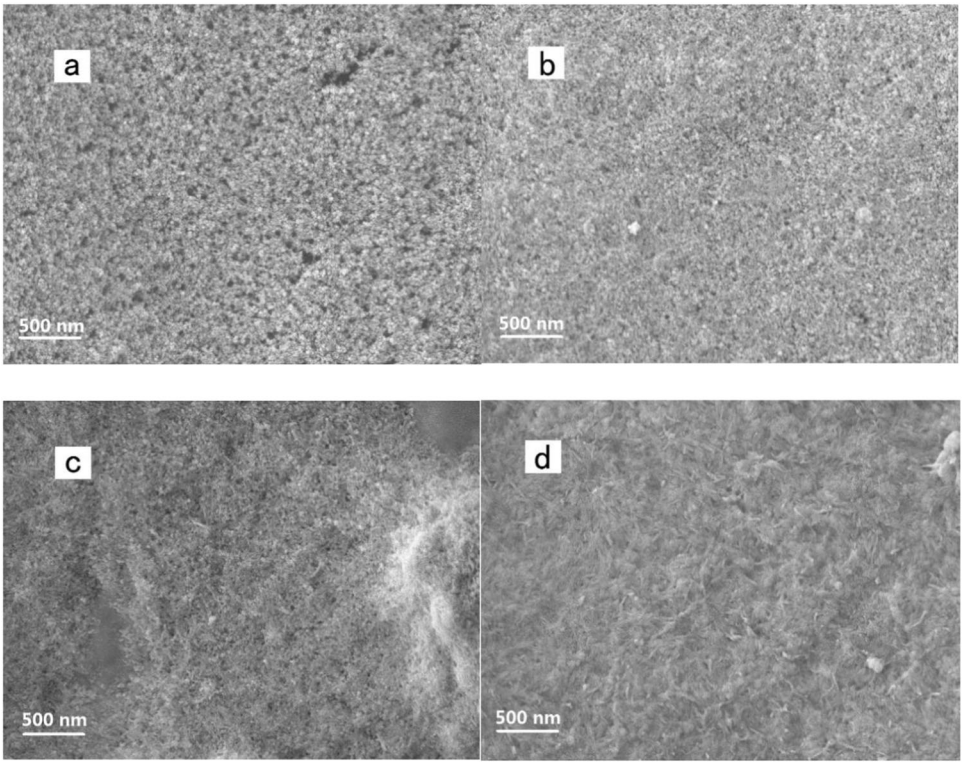

Fig. 6 SEM images of $AlCl_3$-HA flocs with different ages (×30,000): **a** 1 day, **b** 5 days, **c** 10 days, **d** 20 days

there was no crystallization process for all of the precipitate sludge within an aging time of 10 days (Fig. 5a, b, c).

In contrast, the formation of crystalline bayerite was evident after several days for the Al-HA sludges from the XRD profiles (Fig. 5d, e, f). The peak intensities of the crystalline phase for all three flocs/sludges increased with age (from 1 to 10 days), indicating the gradual change of the amorphous solids to more ordered phases.[49] These results suggested that the presence of HA accelerated the crystallization of all three Al-HA flocs, probably leading to an increase of TMP development. It is believed that the loss of water from the nanoparticles at room temperature led to a dramatic structural variation, with the disordered amorphous structure transforming into a more crystalline structure.[50] This would indicate that the morphology of the cake layer was composed of different degrees of crystallization, increasing from the inner to outer parts of the cake layer on the membrane surface. This variation in floc structure was confirmed visually by SEM imaging for $AlCl_3$-HA flocs of different ages.

SEM of flocs with different ages

In order to confirm that the crystallization of $AlCl_3$ precipitate was due to the presence of HA, which induced greater membrane fouling, the flocs with different ages were air-dried and imaged by SEM (Fig. 6). It was evident that the structure of the flocs changed significantly with age. Thus, when newly formed, the flocs consisted of thousands of primary nanoparticles which then reduced in size and bonded together more closely. It is speculated that Brownian motion may allow adjacent particles to rotate through jiggling, until reaching a low-energy configuration through a coherent particle-particle interface. Therefore, rotation of particles within aggregates may be strongly influenced by the short-range interactions between adjacent surfaces.[51] Through these effects, the nano-scale primary particles changed gradually, leading to variations in the floc structure. It was clear from the SEM images that the size of primary nanoparticles reduced and micro-crystallization of flocs occurred over 10 days. At day 20, the $AlCl_3$-HA flocs became rod-like micro-crystals without any nano-scale primary particles evident. Most importantly, the porosity of flocs decreased with age. As the deposited flocs of different ages varied with distance from the membrane surface, it is believed the porosity of the cake layer decreased with increasing proximity to the membrane surface because of the crystallization process.

This study has considered how different Al coagulants ($AlCl_3$, $PACl_{15}$ and $PACl_{25}$), used as pre-treatment before ultrafiltration, affected the nature of the cake layer on the UF surface and on the membrane fouling as time, with and without the presence of HA. The key conclusions are as follows:

1. Pre-coagulation can mitigate membrane fouling during the ultrafiltration process, but the performance depends on the properties of the coagulants, and particularly the process of floc crystallization. The performance of the three coagulants decreased in the order: $PACl_{15}$ > $PACl_{25}$ > $AlCl_3$, according to the results of TMP development. The worst performance, with $AlCl_3$, was due to smallest primary nanoparticles, a more density and thicker cake layer formed on the membrane surface, compared to the other coagulants, which resulted in a higher resistance to flow.
2. Membrane fouling can be mitigated by decreasing the thickness, and increasing the porosity of the cake layer. PACl flocs with larger sized primary nanoparticle and a lower fractal dimension resulted in less membrane fouling.
3. SEM images of flocs with different ages demonstrated that they were composed of thousands of primary nanoparticles when newly formed, but then became smaller and bonded together more closely, and changed in nature through crystallization with the flocs becoming rod-like micro-crystals.
4. Although the size of primary nanoparticles was larger and the porosity of the cake layer was greater in the presence of HA,

the HA induced much greater membrane fouling, through accelerating the crystallization of the cake layer.

METHODS

Synthetic raw water and coagulant

The raw (feed) water used in this study was tap water (with residual chorine removed by standing for 24 h) or tap water mixed with 5 mg/L humic acid solution (2S101H, International Humic Acid Substance Society, USA). Tap water (London, United Kingdom) was chosen here to provide sufficient background ions and alkalinity. We used this model waters to simulate the actual drinking water as much as possible. The properties of both waters are listed in Tables 1 and 2, respectively.

PACls with different OH/Al ratio (B value) were used as coagulants in this study. An alkali titration method was used to prepare these at room temperature,[52] and specific B values of 0, 1.5, and 2.5 were produced, and denoted as $PACl_0$ ($AlCl_3$), $PACl_{15}$, and $PACl_{25}$, respectively. $PACl_{15}$ and $PACl_{25}$ contain around 50 and 90% Al_b/Al_{13}, respectively. In all cases, the concentration of stock PACl solutions were prepared at 0.1 mol/L.

Coagulation and membrane filtration system

Four mini pilot-scale coagulation-UF (CUF) systems were operated in parallel, corresponding to pre-treatment with three species of Al coagulants ($PACl_0$ ($AlCl_3$), $PACl_{15}$, and $PACl_{25}$), and one without pre-coagulation; this experimental arrangement is illustrated in the supporting information (Fig. S1). The concentration of PACls was set at 0.1 mM, which was established as the dose needed to remove most of the HA in pre-tests. Further details of the test procedures and the hollow-fiber UF membrane module are provided in the supporting information. The membrane systems were operated continuously at constant flux (20 L/(m^2h) for a period of 18 days, with for a single washing event (by sponge) at day 13. Further information could be found in the supporting information.

Other methods

A Malvern Mastersizer 2000 (Malvern, U.K.) was used to determine the particle size distribution and the fractal dimension (D_f) of particles/flocs, which were sampled from the three membrane tanks employing pre-coagulation, as used in other studies.[53,54] In addition, dynamic light scattering (Zetasizer, Nano ZS90, Malvern Instruments, PA) was used to measure the size of nano-scale colloidal suspensions (after 0.45 µm membrane). UV absorbance at the wavelength of 254 nm (UV_{254}) and DOC were determined by an ultraviolet/visible spectrometer (U-3010 Hitachi High-Technolgies Co., Japan) and total organic carbon (TOC) analyzer (TOC-V_{CPH}, Shimadzu, Japan) respectively. Turbidity was measured by turbidimeter (2100N, HACH, USA) and ICP-OES (Agilent 5110, USA) was used to determine residual Al concentrations. The crystalline structure of the flocs/precipitates was examined by X-ray diffraction (XRD, Rigaku UltimaIV, Cu-Kα radiation, 45 kV, 50 mA, Japan). Samples of fouled membranes were cut and coated by a Cr sputter, and were imaged by scanning electron microscopy (SEM; JSM7401F, JEDL, Japan).

DATA AVAILABILITY

The data that support the findings of this study are available as supplementary information.

ACKNOWLEDGEMENTS

This research reported in this paper was supported by the Engineering and Physical Sciences Research Council (grant number EP/N010124/1) and a Marie Curie International Incoming Fellowship (FP7-PEOPLE-2012-IIF-328867) within the 7th European Community Framework Programme. This work was also supported by the National Natural Science Foundation of China (Grants 51138008 and 51108444) and Thousand Youth Talents Plan of China.

AUTHOR CONTRIBUTIONS

W.Y. and N.G. have contributed to the design of the study and the critical revision of the article. M.L., X.Z., and W.Y. did the experiments, analyzed the data, prepared figures and drafted the article. N.G., J.Q., and W.Y. finished the final version of the manuscript.

ADDITIONAL INFORMATION

Supplementary information accompanies the paper on the *npj Clean Water* website (https://doi.org/10.1038/s41545-019-0040-3).

Competing interests: The authors declare no competing interests.

Publisher's note: Springer Nature remains neutral with regard to jurisdictional claims in published maps and institutional affiliations.

REFERENCES

1. Kim, E. S., Liu, Y. & El-Din, M. G. Evaluation of membrane fouling for in-line filtration of oil sands process-affected water: the effects of pretreatment conditions. *Environ. Sci. Technol.* **46**, 2877–2884 (2012).
2. Tian, J. Y. et al. Applying ultraviolet/persulfate (UV/PS) pre-oxidation for controlling ultrafiltration membrane fouling by natural organic matter (NOM) in surface water. *Water Res.* **132**, 190–199 (2018).
3. Yu, W. Z., Liu, T., Crawshaw, J., Liu, T. & Graham, N. Ultrafiltration and nanofiltration membrane fouling by natural organic matter: mechanisms and mitigation by pre-ozonation and pH. *Water Res.* **139**, 353–362 (2018).
4. Yu, W. Z., Zhang, D. Z. & Graham, N. J. D. Membrane fouling by extracellular polymeric substances after ozone pre-treatment: variation of nano-particles size. *Water Res.* **120**, 146–155 (2017).
5. Yu, W. Z., Xu, L., Qu, J. H. & Graham, N. Investigation of pre-coagulation and powder activate carbon adsorption on ultrafiltration membrane fouling. *J. Membr. Sci.* **459**, 157–168 (2014).
6. Cai, Z. X. & Benjamin, M. M. NOM fractionation and fouling of low-pressure membranes in microgranular adsorptive filtration. *Environ. Sci. Technol.* **45**, 8935–8940 (2011).
7. Liu, T. et al. Mitigation of NOM fouling of ultrafiltration membranes by pre-deposited heated aluminum oxide particles with different crystallinity. *J. Membr. Sci.* **544**, 359–367 (2017).
8. Huang, H. O., Cho, H. H., Jacangelo, J. G. & Schwab, K. J. Mechanisms of membrane fouling control by integrated magnetic ion exchange and coagulation. *Environ. Sci. Technol.* **46**, 10711–10717 (2012).
9. Hazrati, H., Jahanbakhshi, N. & Rostamizadeh, M. Fouling reduction in the membrane bioreactor using synthesized zeolite nano-adsorbents. *J. Membr. Sci.* **555**, 455–462 (2018).
10. Humbert, H., Gallard, H. & Croue, J. P. A polishing hybrid AER/UF membrane process for the treatment of a high DOC content surface water. *Water Res.* **46**, 1093–1100 (2012).
11. Wang, J. & Wang, X. C. Ultrafiltration with in-line coagulation for the removal of natural humic acid and membrane fouling mechanism. *J. Environ. Sci. China* **18**, 880–884 (2006).
12. Park, J., Takizawa, S., Katayama, H. & Ohgaki, S. Biofilter pretreatment for the control of microfiltration membrane fouling. *2nd World Water Congr.: Drink. Water Treat.* **2**, 193–199 (2002).
13. Myat, D. T. et al. Characterisation of organic matter in IX and PACl treated wastewater in relation to the fouling of a hydrophobic polypropylene membrane. *Water Res.* **46**, 5151–5164 (2012).
14. Yu, W. Z., Campos, L. C. & Graham, N. Application of pulsed UV-irradiation and pre-coagulation to control ultrafiltration membrane fouling in the treatment of micro-polluted surface water. *Water Res.* **107**, 83–92 (2016).
15. Liu, B. et al. Membrane fouling and rejection of organics during algae-laden water treatment using ultrafiltration: a comparison between in situ pretreatment with Fe(II)/Persulfate and ozone. *Environ. Sci. Technol.* **52**, 765–774 (2018).
16. Hatt, J. W., Germain, E. & Judd, S. J. Precoagulation-microfiltration for wastewater reuse. *Water Res.* **45**, 6471–6478 (2011).
17. Huang, B. C., Guan, Y. F., Chen, W. & Yu, H. Q. Membrane fouling characteristics and mitigation in a coagulation-assisted microfiltration process for municipal wastewater pretreatment. *Water Res.* **123**, 216–223 (2017).
18. Ly, Q. V., Nghiem, L. D., Cho, J. & Hur, J. Insights into the roles of recently developed coagulants as pretreatment to remove effluent organic matter for membrane fouling mitigation. *J. Membr. Sci.* **564**, 643–652 (2018).
19. Fan, L. H., Nguyen, T., Roddick, F. A. & Harris, J. L. Low-pressure membrane filtration of secondary effluent in water reuse: Pre-treatment for fouling reduction. *J. Membr. Sci.* **320**, 135–142 (2008).
20. Tang, S. Y., Zhang, Z. H. & Zhang, X. H. Coupling in-situ ozonation with ferric chloride addition for ceramic ultrafiltration membrane fouling mitigation in wastewater treatment: Quantitative fouling analysis. *J. Membr. Sci.* **555**, 307–317 (2018).
21. Lahoussine-Turcaud, V., Wiesner, M. R., Bottero, J.-Y. & Mallevialle, J. Coagulation pretreatment for ultrafiltration of a surface water. *Am. Water Works Assoc. J.* **82**, 76–81 (1990).

22. Mao, R. R. et al. Impact of enhanced coagulation ways on flocs properties and membrane fouling: Increasing dosage and applying new composite coagulant. *Desalination* **314**, 161–168 (2013).
23. Barbot, E., Moustier, S., Bottero, J. Y. & Moulin, P. Coagulation and ultrafiltration: understanding of the key parameters of the hybrid process. *J. Membr. Sci.* **325**, 520–527 (2008).
24. Konieczny, K., Sakol, D., Plonka, J., Rajca, M. & Bodzek, M. Coagulation-ultrafiltration system for river water treatment. *Desalination* **240**, 151–159 (2009).
25. Citulski, J., Farahbakhsh, K., Kent, F. & Zhou, H. D. The impact of in-line coagulant addition on fouling potential of secondary effluent at a pilot-scale immersed ultrafiltration plant. *J. Membr. Sci.* **325**, 311–318 (2008).
26. Kabsch-Korbutowicz, M. Effect of Al coagulant type on natural organic matter removal efficiency in coagulation/ultrafiltration process. *Desalination* **185**, 327–333 (2005).
27. Zhao, B., Wang, D., Li, T., Chow, C. W. K. & Huang, C. Influence of floc structure on coagulation–microfiltration performance: effect of Al speciation characteristics of PACls. *Sep Purif. Technol.* **72**, 22–27 (2010).
28. Zheng, X., Plume, S., Ernst, M., Croue, J. P. & Jekel, M. In-line coagulation prior to UF of treated domestic wastewater - foulants removal, fouling control and phosphorus removal. *J. Membr. Sci.* **403**, 129–139 (2012).
29. Xu, W. Y. & Gao, B. Y. Effect of shear conditions on floc properties and membrane fouling in coagulation/ultrafiltration hybrid process-The significance of Al-b species. *J. Membr. Sci.* **415**, 153–160 (2012).
30. Wang, J., Guan, J., Santiwong, S. R. & Waite, T. D. Characterization of floc size and structure under different monomer and polymer coagulants on microfiltration membrane fouling. *J. Membr. Sci.* **321**, 132–138 (2008).
31. Ho, C. C. & Zydney, A. L. A combined pore blockage and cake filtration model for protein fouling during microfiltration. *J. Colloid Inter. Sci.* **232**, 389–399 (2000).
32. Bagga, A., Chellam, S. & Clifford, D. A. Evaluation of iron chemical coagulation and electrocoagulation pretreatment for surface water microfiltration. *J. Membr. Sci.* **309**, 82–93 (2008).
33. Yu, W. Z. et al. Influence of flocs breakage process on submerged ultrafiltration membrane fouling. *J. Membr. Sci.* **385**, 194–199 (2011).
34. Antelmi, D., Cabane, B., Meireles, M. & Aimar, P. Cake collapse in pressure filtration. *Langmuir* **17**, 7137–7144 (2001).
35. Park, P. K., Lee, C. H. & Lee, S. Determination of cake porosity using image analysis in a coagulation-microfiltration system. *J. Membr. Sci.* **293**, 66–72 (2007).
36. Lee, J. D. et al. Effect of coagulation conditions on membrane filtration characteristics in coagulation-microfiltration process for water treatment. *Environ. Sci. Technol.* **34**, 3780–3788 (2000).
37. Wang, J., Guan, J., Santiwong, S. R. & Waite, T. D. Effect of aggregate characteristics under different coagulation mechanisms on microfiltration membrane fouling. *Desalination* **258**, 19–27 (2010).
38. Yu, W. Z., Xu, L., Lei, K. Y. & Gregory, J. Effect of crystallization of settled aluminum hydroxide precipitate on "dissolved Al". *Water Res.* **143**, 346–354 (2018).
39. Rousseaux, J. M., Weisbecker, P., Muhr, H. & Plasari, E. Aging of precipitated amorphous alumina gel. *Ind. Eng. Chem. Res.* **41**, 6059–6069 (2002).
40. Hayden P. L., Rubin A. J. In aqueous environmental chemistry of metals. (ed. Rubin A. J.) 317–381 (Ann Arbor Science Publishers Inc, Ann Arbor, Michigan, 1974).
41. de Vicente, I., Huang, P., Andersen, F. O. & Jensen, H. S. Phosphate adsorption by fresh and aged aluminum hydroxide. Consequences for lake restoration. *Environ. Sci. Technol.* **42**, 6650–6655 (2008).
42. Duffy, S. J. & Vanloon, G. W. Characterization of amorphous aluminum hydroxide by the Ferron method. *Environ. Sci. Technol.* **28**, 1950–1956 (1994).
43. Marboe, E. C. & Bentur, S. A new interpretation of the aging of aluminum hydroxide gel. *Silic. Ind.* **26**, 389–399 (1961).
44. Bardossy, G. & White, J. L. Carbonate inhibits the crystallization of aluminum hydroxide in bauxite. *Science* **203**, 355–356 (1979).
45. Mayer, T. D. & Jarrell, W. M. Phosphorus sorption during iron(II) oxidation in the presence of dissolved silica. *Water Res.* **34**, 3949–3956 (2000).
46. Lin, J. L., Huang, C. P., Chin, C. J. M. & Pan, J. R. The origin of Al(OH)(3)-rich and Al-13-aggregate flocs composition in PACl coagulation. *Water Res.* **43**, 4285–4295 (2009).
47. Yu, W. Z., Graham, N., Liu, H. J. & Qu, J. H. Comparison of FeCl3 and alum pre-treatment on UF membrane fouling. *Chem. Eng. J.* **234**, 158–165 (2013).
48. Howe, K. J. & Clark, M. M. Fouling of microfiltration and ultrafiltration membranes by natural waters. *Environ. Sci. Technol.* **36**, 3571–3576 (2002).
49. Berkowitz, J., Anderson, M. A. & Graham, R. C. Laboratory investigation of aluminum solubility and solid-phase properties following alum treatment of lake waters. *Water Res.* **39**, 3918–3928 (2005).
50. Zhang, H. Z., Gilbert, B., Huang, F. & Banfield, J. F. Water-driven structure transformation in nanoparticles at room temperature. *Nature* **424**, 1025–1029 (2003).
51. Zhu, H. Sintering processes of two nanoparticles: a study by molecular dynamics simulations. *Philos. Mag. Lett.* **73**, 27–33 (1996).
52. Yu, W. Z., Gregory, J. & Campos, L. C. Breakage and re-growth of flocs: Effect of additional doses of coagulant species. *Water Res.* **45**, 6718–6724 (2011).
53. Yu, W. Z., Liu, H. J., Liu, T., Liu, R. P. & Qu, J. H. Comparison of submerged coagulation and traditional coagulation on membrane fouling: Effect of active flocs. *Desalination* **309**, 11–17 (2013).
54. Jarvis, P., Jefferson, B. & Parsons, S. A. Breakage, regrowth, and fractal nature of natural organic matter flocs. *Environ. Sci. Technol.* **39**, 2307–2314 (2005).